Article

Intercomparison of Leaf Area Index Products for a Gradient of Sub-Humid to Arid Environments in West Africa

Ursula Gessner *, Markus Niklaus, Claudia Kuenzer and Stefan Dech

German Remote Sensing Data Center (DFD), German Aerospace Center (DLR), Muenchner Strasse 20, 82234 Wessling, Germany; E-Mails: markus.niklaus@dlr.de (M.N.); claudia.kuenzer@dlr.de (C.K.); stefan.dech@dlr.de (S.D.)

* Author to whom correspondence should be addressed; E-Mail: ursula.gessner@dlr.de; Tel.: +49-8153-281-250; Fax: +49-8153-281-458.

Abstract: The Leaf Area Index (LAI) is a key variable in many land surface and climate modeling studies. To date, a number of LAI datasets have been developed based on time series of medium resolution optical remote sensing observations. Global validation exercises show the high value of these datasets, but at the same time they point out shortcomings, particularly in the presence of persistent cloud coverage and dense vegetation. For regional modeling studies, the choice of an ideal LAI input dataset is not straightforward as global validation, and intercomparison studies do not necessarily allow conclusions on data quality at regional scale. This paper provides a comprehensive relative intercomparison of four freely available LAI products for a wide gradient of ecosystems in Africa. The region of investigation, West Africa, comprises typical African sub-humid to arid landscapes. The selected LAI time series are the Satellite Pour l'Observation de la Terre-VEGETATION (SPOT-VGT)-based Carbon Cycle and Change in Land Observational Products from an Ensemble of Satellites (CYCLOPES) LAI, the SPOT-VGT-based Bio-geophysical Parameters (BioPar) LAI product GEOV1, the Moderate Resolution Imaging Spectroradiometer (MODIS) product MOD15A2, and the Meteosat-SEVIRI-based Satellite Application Facility on Land Surface Analysis (LSA-SAF) LAI. The comparative analyses focus on data gap occurrence, on the consistency of temporal LAI profiles, on their ability to adequately reproduce the phenological cycle and on the plausibility of LAI magnitudes for major land cover types in West Africa. A detailed quantitative validation of the LAI datasets, however, was not possible due to insufficient ground LAI measurements in the study region.

1. Introduction

The terrestrial vegetation plays an important role for land surface fluxes of water and energy. Processes, such as infiltration and interception of rainfall, absorption of radiation and photosynthesis are influenced by vegetation and, in particular, by the amount of foliage in plant canopies. A key variable for describing the leaf canopy is the Leaf Area Index (LAI). LAI is defined as the one-sided area of green leaves per unit ground area [1]. Land surface and climate modeling approaches usually require consistent LAI datasets of regional to global coverage [2–5]. This kind of datasets can be created only from large area optical remote sensing observations that are acquired at a medium spatial resolution (250 m–8 km) and at high temporal frequencies. During recent years, a number of LAI products have been developed for example from NOAA-AVHRR (Advanced Very High Resolution Radiometer), MODIS (Moderate Resolution Imaging Spectroradiometer), SEVIRI (Spinning Enhanced Visible and Infrared Imager), and SPOT-VGT (Satellite Pour l'Observation de la Terre-VEGETATION) data.

Global and regional validation exercises emphasize the high value of these remote sensing based LAI datasets [6–16]. At the same time they indicate specific problems, for example in regions of high cloud cover or dense vegetation cover where observations reach saturation [9–11,16] or in areas where the land cover classifications used for LAI retrieval show low accuracies [17]. For several reasons, however, the currently existing validation and intercomparison studies do not provide sufficient generality to draw conclusions on product quality at regional scale [10]. Global validation exercises typically use a well distributed set of reference sites that is representative at global scale [6,7,10]. At regional scale however, the number and representativeness of the considered reference sites is frequently insufficient for meaningful conclusions. Validation studies with a regional focus in contrast allow for an in depth assessment of product quality but results are usually not transferable to other areas [8,9,11–15]. Another drawback of existing validation and intercomparison exercises is that recent LAI products such as the BioPar (Bio-geophysical Parameters) LAI product GEOV1 [18] and the SEVIRI-based product of the Satellite Application Facility on Land Surface Analysis (LSA-SAF) [19,20] are not yet considered. Thus, choosing the best suited LAI dataset for regional modeling studies is not straightforward. In order to enhance the understanding of existing LAI products for users, there is a need to complement global validation and intercomparison studies with further regional investigations.

Also for the African continent, valuable validation and intercomparison studies of LAI products are available which either focus on single LAI products or are limited to single ecosystems [9,13,21]. The objective of this paper is to provide a comprehensive overview of freely available, up to date LAI products for a wide gradient of ecosystems in Africa. As study region, we select West Africa which encompasses sub-humid to arid environments and thus comprises the majority of typical African biomes. The investigated LAI datasets are the SPOT-VGT-based CYCLOPES (Carbon Cycle and Change in Land Observational Products from an Ensemble of Satellites) LAI [22], the SPOT-VGT-based BioPar LAI product GEOV1 [18], the MODIS standard product MOD15A2, collection 5 [23,24], and the Meteosat-SEVIRI-based LAI of the LSA-SAF [19,20]. The comparative
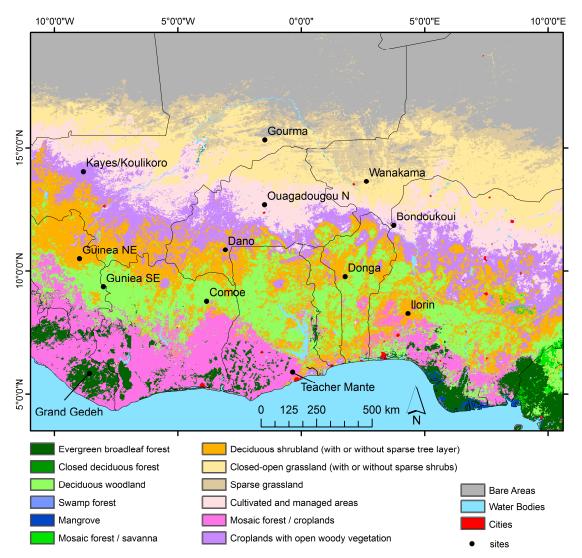
analyses consider aspects that are of relevance for the applicability of LAI products in regional land surface and climate modeling studies. In particular we focus on the spatio-temporal presence of data gaps, as well as on the consistency of the temporal LAI profiles, their ability to reproduce vegetation phenology and the plausibility of LAI magnitudes for major land cover types in West Africa.

2. Material and Methods

2.1. Study Region

The product comparison is conducted for the region of West Africa (10°W–10°E, 20°N–4°N). West Africa is characterized by a strong rainfall gradient ranging from approximately 100 mm/year in the north to 2000 mm/year in the south. Mean temperatures vary between 26 °C and more than 30 °C. The West African vegetation includes major African biomes like evergreen rainforests in the south, woodland, shrubland and grassland savannas as well as sparsely vegetated areas and deserts in the north (Figure 1). Today, vegetation cover is considerably influenced by land use which has led to deforestation, to expansion of agricultural land and to an elevated fire frequency.

Figure 1. The West African study region, its land cover (GLC2000, [25]) and the sites selected for detailed analyses.

2.2. LAI Datasets

Four freely available LAI time series products were compared in this study, which are potential input datasets for land surface and climate models. Table 1 gives an overview of these datasets and of their main characteristics.

Table 1. Basic characteristics of the investigated LAI datasets.

Product	Spatial Resolution	Temporal Resolution	Sensor	Algorithm	Temporal Coverage	Reference	Source
CYCLOPES	1km	10 days/30 days	SPOT-VGT	RTM, NN	1999–2007	[22]	[26]
MOD15A2 (collection 5)	1km	8 days	MODIS-TERRA	RTM, LUT	2000–today	[23,24,27]	[28]
GEOV1	1km	10 days/30 days	SPOT-VGT	NN	1999–today	[18]	[29]
LSA-SAF	3km	daily	MSG-SEVIRI	SMA, SEM	2006–today	[19,20]	[30]

RTM: radiative transfer model; NN: neural networks; LUT: look up tables; SMA: spectral mixture analysis; SEM: semi-empirical model.

2.2.1. CYCLOPES LAI

The CYCLOPES LAI time series has been developed in the EU/FP5 project CYCLOPES by Cnes, CNRM, Inra and Noveltis and is based on daily observations of the SPOT-VGT sensor. Preprocessing of VGT data includes radiometric calibration, cloud screening, atmospheric correction and BRDF normalization. The LAI derivation is based on the inversion of a radiative transfer model (PROSPECT+SAIL) [31]. In this model, the leaves of a canopy are assumed to be randomly distributed in space. Clumping is considered partly at landscape scale but not at leaf and canopy level. For model inversion, neural networks are trained over the radiative transfer model simulations. Each dataset is built from 30 days of observations and time series are provided at a 10-day sampling interval where observations closer to the nominal date are weighted stronger than those earlier or later in time. CYCLOPES LAI data is available for the years 1999–2007 at a spatial resolution of 1 km. A detailed description of the methodology for CYCLOPES LAI derivation can be found in [22].

2.2.2. MOD15A2 LAI

The MODIS land product MOD15A2 (collection 5) provides global time series of LAI derived from daily MODIS-TERRA data. The main algorithm of the MODIS product is based on a look up table which is generated using a 3D radiative transfer model. A structural biome map is used for defining the expected range of vegetation structure and soil patterns when modeling the bi-directional reflectance factors (BRFs). Modeled and observed BRFs are compared and those solutions are accepted where the residuals are smaller than biome-related levels of model and observation uncertainty. Finally the average LAI of all accepted solutions is calculated. The algorithm accounts for clumping at leaf, canopy and partly at landscape scale. In case the main algorithm fails, a backup method is used. This backup method relies on biome-specific relationships between vegetation indices and LAI. MOD15A2 is

available for the years 2000 until today. Data is provided in an 8-day sampling interval at a spatial resolution of 1 km. For further details on the MODIS LAI algorithm we refer to [23,24,27].

2.2.3. GEOV1 LAI

The global BioPar LAI product GEOV1, developed in the framework of the EU project Geoland2, is derived from daily SPOT-VGT top of canopy normalized reflectances. LAI estimation is based on a neural network. The training database for the neural network is built from subsets of the LAI datasets MODIS C5 and CYCLOPES for the years 2003–2004 at BELMANIP (Benchmark Land Multisite Analysis and Intercomparison of Products) validation sites [32]. The GEOV1 LAI accounts for clumping at canopy and leaf scales. Each dataset is created from 30 days of SPOT-VGT data using the same weighting function as for the CYCLOPES data, and the time series is available at a 10-day sampling interval. GEOV1 data is available for the years 1999 until today at a spatial resolution of 1 km. The GEOV1 method is described in detail by [18].

2.2.4. LSA-SAF LAI

The LSA-SAF LAI product is delineated from data of SEVIRI on board of Meteosat Second Generation (MSG). SEVIRI provides data with a repeat cycle of 15 min at a spatial resolution of 3 km at nadir. LSA-SAF LAI retrieval is based on fractional vegetation cover information that is derived using an optimized spectral mixture analysis. A semi-empirical approach is then applied to estimate LAI from fractional vegetation cover [33]. Here, a tractable physical model allows estimating the interception of solar direct irradiance by vegetation canopies with random foliage distribution. The clumping effect is corrected using an empirical land cover dependent clumping index. Clumping is assumed to be homogeneous within land cover classes of the GLC2000 and its magnitude is estimated based on global POLDER (Polarization and Directionality of Earth Reflectance) multiangular data [34]. A detailed description on the methodological approach for retrieving the LSA-SAF LAI dataset can be found in [19,20].

2.3. Intercomparison of LAI Datasets

The LAI datasets are compared for the region of West Africa and for the years 2006–2007. Due to common data availability during this period, it was possible to analyze all four LAI datasets. Furthermore, the years 2006 and 2007 are a representative subset of the last decades in terms of rainfall. The consistency of the LAI products is first evaluated by examining the frequency and duration of data gaps. Subsequently, the magnitudes of LAI values are compared and the capability of the products to reproduce the seasonal development of vegetation is evaluated. In this context, we investigate region-wide spatial LAI patterns, average LAI characteristics of typical land cover types in West Africa and local LAI profiles at 13 selected sites of 3 km × 3 km (Table 2, Figure 1). For the land cover related analyses, we chose the land cover map GLC2000 [25] that is shown in Figure 1. GLC2000 was found to characterize biophysical properties more precisely than a range of other land cover maps [35] and it is frequently recommended and used as an input dataset for land surface models [36–39]. The sites selected for local profile analyses comprise locations of the BELMANIP [32] and BELMANIP-2 [40] networks which were established for the evaluation of

biophysical land surface datasets, and locations of the VALERI (Validation of Land European Remote sensing Instruments) project [41]. The sites were complemented by two additional locations to better cover the predominant land cover types in West Africa.

Table 2. Basic characteristics of the sites that are selected for detailed analyses. For the purpose of clarity, a name was assigned to each of the sites even if the site did not have a name in the BELMANIP database.

Name	Lat.	Lon.	Land Cover (GLC2000)	Network/Origin
Bondoukoui	11.85	3.75	Cultivated and managed areas	BELMANIP
Comoe	8.77	−3.83	Deciduous woodland	additional
Dano	10.86	−3.08	Deciduous shrubland (with or without sparse tree layer)	BELMANIP
Donga	9.77	1.78	Deciduous shrubland (with or without sparse tree layer)	VALERI
Gourma	15.32	−1.56	Closed-open grassland	BELMANIP/VALERI
Grand Gedeh	5.85	−8.58	Evergreen broadleaf forest	BELMANIP 2
Guinea NE	10.50	−8.99	Deciduous shrubland (with or without sparse tree layer)	BELMANIP 2
Guinea SE	9.35	−8.02	Deciduous woodland	BELMANIP 2
Ilorin	8.28	4.32	Deciduous shrubland (with or without sparse tree layer)	BELMANIP 2
Kayes/Koulikoro	14.04	−8.82	Croplands with open woody vegetation	BELMANIP 2
Ouagadougou N	12.69	−1.49	Cultivated and managed areas	BELMANIP 2
Teacher Mante	5.90	−0.35	Mosaic forest/croplands	additional
Wankama	13.64	2.64	Closed-open grassland	BELMANIP/VALERI

In situ LAI measurements for the study region are only available for dates prior to the period of investigation (2006–2007), when LSA-SAF LAI data was not yet available. Therefore, a direct and spatially explicit comparison of ground measurements with the presented LAI products is not possible. However, we consulted several earlier field surveys in sub-Saharan Africa of the northern hemisphere and Amazonia (Table 3) for a rough evaluation of the land cover related LAI distributions of the selected products.

Table 3. LAI estimates in northern hemispherical sub-Saharan Africa and Amazonia based on *in situ* measurements and high resolution maps.

Name	Country	Land Cover	Date	LAI	Source
Kakamega	Kenya	evergreen broadleaf forest	Oct.–Nov. 2004	3.95–7.4	[13], *in situ*
Budongo	Uganda	evergreen broadleaf forest	Oct. 2005	6.0–7.4	[13], *in situ*
Tapajós	Brazil	evergreen broadleaf forest (primary forest)	Oct. 2002	3.25–5.1	[11,12], *in situ*
GlobalAVG	global	evergreen broadleaf forest	multiannual	4.9	[42], *in situ* (average)
Donga	Benin	deciduous shrubland	Jun. 2005	1.8	[41], high resolution map
Wankama	Niger	closed-open grassland	Jun. 2005	0.1	[41], high resolution map
Gourma	Mali	closed-open grassland	Aug.–Sep. 2000	0.41–0.84	[41], *in situ*
Gourma	Mali	closed-open grassland	Sep.–Oct. 2001	0.91–1.28	[41], *in situ*
Dahra	Senegal	grassland	Sep. 2001	1.5–2.5	[9], *in situ*
Dahra, Tessekre North, Tessekre South	Senegal	grassland	Jul.–Sep. 2002	0–0.75	[9], *in situ*

The original temporal and spatial resolution of the LAI products was kept during intercomparison (unless indicated differently) to allow a better evaluation of advantages and drawbacks of the individual datasets. For the MOD15A2 LAI product, the analyses were restricted to data that is based on the main algorithm. Any data estimated by the backup algorithm was not considered and masked as invalid, as other studies have shown a questionable reliability of this algorithm [7,43].

3. Results

3.1. Data Gaps

The spatial patterns of data gap frequency (Figure 2(a–c)) and maximum gap length (Figure 2(d–f)) for the years 2006–2007 are illustrated in Figure 2. LSA-SAF LAI is not displayed as this product does not show any spatial variations in missing data. In case a time slice of LSA-SAF LAI is available, this dataset is complete without any gaps.
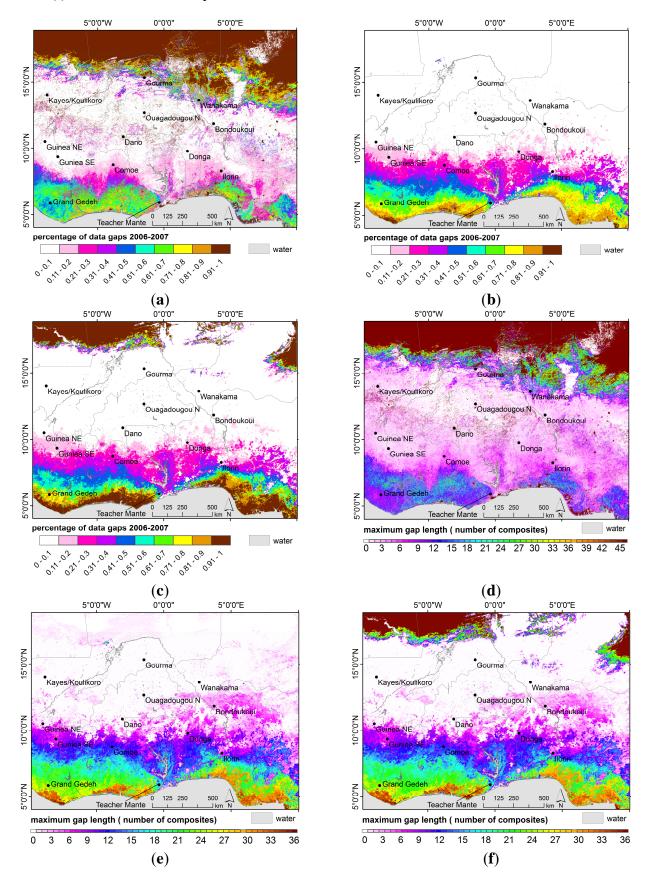
In CYCLOPES and GEOV1 data, we observe 0%–20% of data gaps within the central zone of the study region between 15°N and 10°N. Similar conditions are found in the MODIS dataset between 13°N and 10°N (Figure 2(a–c)). South of 10°N, data gaps increase with decreasing latitude. This latitudinal pattern refers to the increasing precipitation and thus increasing cloud coverage towards the Inner-Tropical Convergence Zone (ITCZ). North of 15°N and 13°N, extensive and persistent data gaps occur in the CYCLOPES and MODIS datasets, respectively. The reason for these gaps is that in CYCLOPES and MOD15A2 products, LAI is generally not processed for certain arid land cover types like barren or sparsely vegetated areas where vegetation cover is assumed to be negligible [23,44]. The area of missing data, however, is not the same for both products as they do not rely on the same land cover dataset.

The maximum length of data gaps shows similar spatial patterns (Figure 2(d–f)). In the northern zone, CYCLOPES and MODIS LAI data are missing for the complete 2006–2007 period while in the central zone, data gaps are shorter than 1.5 months. South of 10°N, the duration of data gaps increases with decreasing latitude. In the coastal areas, data is unavailable for up to 6–7 month for MODIS and 10–12 months for CYCLOPES and GEOV1 data.

The seasonal variations of data gaps for land pixels during 2006–2007 are displayed in Figure 3 for the humid zone south of 10°N that turned out to be most significantly affected by data gaps (*cf.* Figure 2). Data gaps in the zone north of 13°N are less relevant as they are mainly located in areas where vegetation cover is absent or at least of marginal importance.

Regarding the LSA-SAF LAI dataset, 36% of the daily data is missing in 2006 (Figure 3, rose color). In 2007, data gaps in this product constitute 3% of the data. A low level of 1%–7% of missing data is also found later in 2008–2012 (not displayed), so that the 2007 situation can be considered as the standard situation for the LSA-SAF LAI dataset. Furthermore, data gaps in the LSA-SAF product do not accumulate during a certain season, so that even in the highly gap affected year 2006, the longest data gap spans only 25 days.

Figure 2. Spatial variation of data gap percentage for (**a**) MOD15A2, (**b**) GEOV1, and (**c**) CYCLOPES, and maximum gap length for (**d**) MOD15A2, (**e**) GEOV1, and (**f**) CYCLOPES for the period 2006–2007.
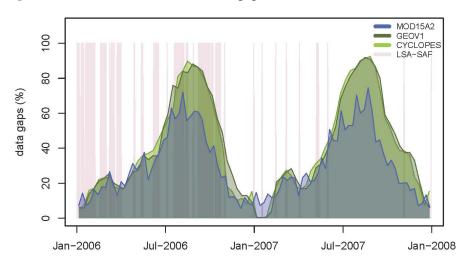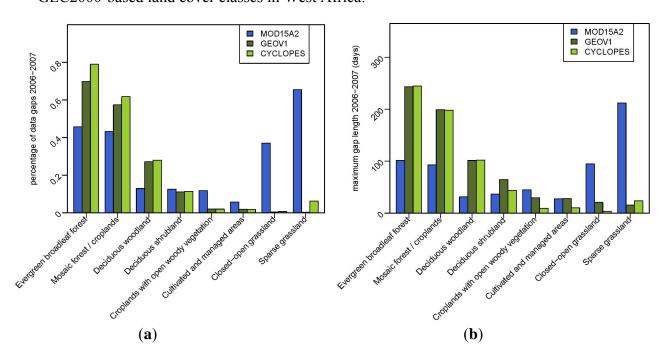
Figure 3. Seasonal variation of data gaps for West Africa south of 10°N.

The latitudinal variations in data gaps lead to strong differences in data availability for the predominant land cover types in West Africa (Figure 4). *Evergreen broadleaved forests* and *forest/cropland mosaics* in the south are heavily affected by missing data. Here, MOD15A2 provides the highest fraction of valid data (*ca.* 55%) and shortest gap lengths (*ca.* 100 days). *Deciduous woodlands* show approximately 10% of missing data in the MODIS LAI dataset and almost 30% in the GEOV1 and CYCLOPES products. In contrast, the availability of MOD15A2 data for the sparsely vegetated land cover types *closed-open grassland* and *sparse grassland* is relatively poor (35%–65% of missing data). Here, CYCLOPES and GEOV1 products show hardly any missing data (<6%). All other land cover classes are characterized by good to intermediate data availability with 2%–10% of data gaps and maximum gap lengths largely shorter than 65 days.

Figure 4. Percentage of data gaps (**a**) and maximum annual gap length (**b**) for predominant, GLC2000-based land cover classes in West Africa.

(**a**)   (**b**)

3.2. LAI Magnitudes and Their Statistical Distributions

The LAI magnitudes of the selected products are first compared for the vegetation phase 2007. For intercomparison, the MOD15A2 8-day composite of 22–29 September was chosen. The mean LSA-SAF LAI was calculated over the same period from the daily datasets. For GEOV1 and CYCLOPES, we selected the 23 and 25 September datasets respectively. These datasets are built from 30 days of VEGETATION observations centered on the nominal date. Observations have higher weights, the closer they are to the nominal date. Thus, it has to be considered that the selected GEOV1 and CYCLOPES datasets represent slightly longer periods than the MODIS and LSA-SAF products.

In Figure 5, the LAI datasets for end of September 2007 are compared in scatter plots. Here, all datasets were scaled to the 3 km × 3 km grid of LSA-SAF LAI by averaging the higher resolution LAI values over the coarser grid cells, in order to allow for a direct pixel-by-pixel comparison. The spatial LAI patterns of end of September 2007 are displayed in Figure 6 at their original spatial resolution. The scatter plots show good agreement between GEOV1, CYCLOPES and LSA-SAF LAI with RMSEs ranging between 0.24 and 0.28 (Figure 5(a–c)). These datasets agree particularly well for LAI values below 2.5. For LAIs above this value, GEOV1 provides higher LAIs than CYCLOPES and LSA-SAF. The respective areas of relative overestimation are mainly located in the *deciduous shrubland* and *deciduous woodland* zones of GLC2000 (compare Figures 6 and 1).
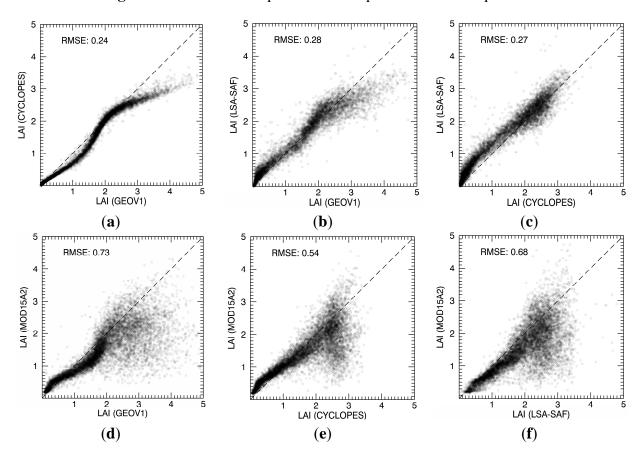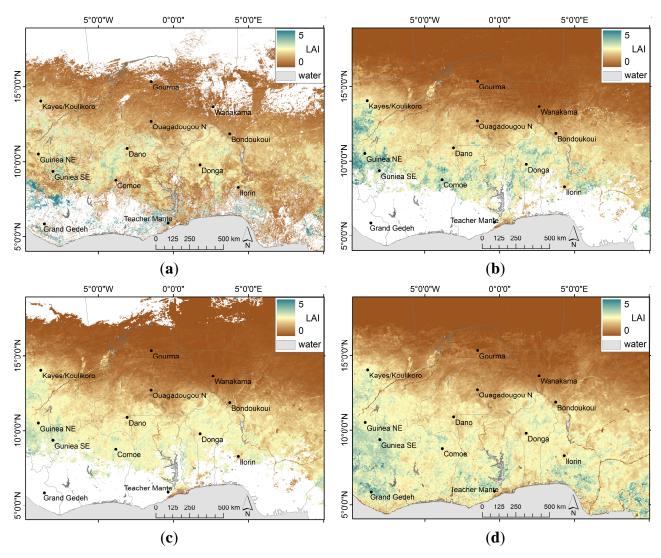
Figure 5. Product *versus* product scatter plots for end of September 2007.

MOD15A2 LAI shows stronger discrepancies with the rest of the LAI products and RMSE range between 0.54 and 0.73 (Figure 5(d–f)). For LAI values below 2, MOD15A2 is in acceptable agreement
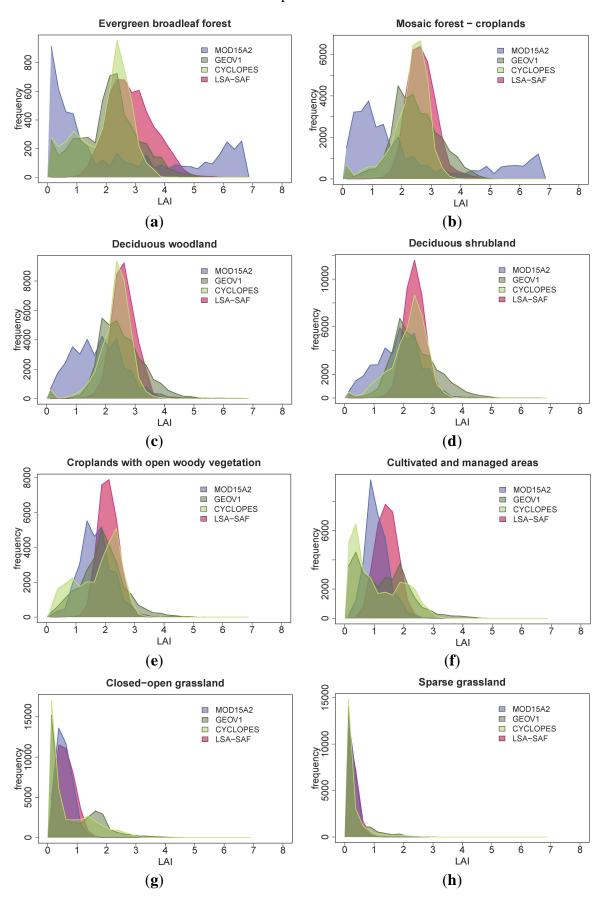
with the other products. The high overall RMSEs are mainly caused by LAI values above 2 where values scatter considerably. Here, MOD15A2 shows a relative underestimation of LAI when compared to the other products. The spatial patterns of LAI (Figure 6(a)) support that this underestimation is related to a decrease of MODIS LAI south of approximately 11°N. GEOV1, CYCLOPES, and LSA-SAF LAI in contrast tend to increase with decreasing latitude. Given the latitudinal distribution of rainfall and land cover types in West Africa, this increase of LAI towards the south is more realistic than the spatial patterns of the MODIS LAI dataset.

Figure 6. LAI for end of September 2007: (**a**) MOD15A2, (**b**) GEOV1, (**c**) CYCLOPES, and (**d**) LSA-SAF.

The statistical distributions of LAI values for the predominant land cover classes of West Africa, as defined by GLC2000, are presented in Figure 7. Again, the histograms show the growing season situation end of September 2007. The selected *in situ* measured and high resolution map based LAI estimates (Table 3) allow for a rough assessment of the adequacy of LAI distributions for some of the presented land cover types.

Figure 7. Statistical distribution of LAI values for predominant, GLC2000-based land cover classes of West Africa for end of September 2007.

(a)

(b)

(c)

(d)

(e)

(f)

(g)

(h)

The *in situ* measurements for *evergreen broadleaf forest* in East Africa vary between 3.95 and 7.4 ([13], Table 3). [42] report global averages from ground measurements of *tropical evergreen broadleaf forests* around 4.9 and [11,12] measured slightly lower LAI values for the Amazonian *evergreen broadleaf forest* between 3.25 and 5.1. The LAI distributions for *evergreen broadleaf forest* in CYCLOPES, GEOV1 and MOD15A2 products are characterized by two peaks (Figure 7(a)). In all three products, a considerable number of pixels show LAI values below 1.5 (CYCLOPES: 29.4%; GEOV1: 26.7%; MOD15A2: 55.3%). These extremely low LAI values could in principle be related to misclassifications in GLC2000. However, the validation of GLC2000 [45] shows only minor commission errors for *evergreen broadleaf forest*: less than 5% of this class erroneously includes non-forest land cover types that could explain LAI values below 1.5. Another reason for the low LAI values could be deforestation that has happened in West Africa since the creation of the land cover map in the year 2000. According to statistics of the Food and Agriculture Organization (FAO), 9.5% of the forests in the study region (Liberia, Ivory Coast, Ghana, Nigeria and Cameroon) have been lost between 2000 and 2007 [46]. Thus, deforestation alone cannot explain the high percentage of low LAI values in the CYCLOPES, GEOV1 and MOD15A2 datasets. A very plausible reason for the frequent low LAI values seems to be an underestimation of LAI due to remaining cloud contamination in the south of West Africa. The second peak in the LAI distributions is found between values of 2–3 for CYCLOPES and GEOV1 and around 6–7 for MOD15A2. Here, MODIS LAI values seem more realistic when compared to *in situ* measurements of [13]. The LAI distribution of the LSA-SAF product for *evergreen broadleaf forest* shows only one peak around 2–3.5. While extremely low values are missing in this product, average LAI values are still below the field measurements in East Africa. For the *mosaic forest-croplands* class (Figure 7(b)), the LAI distributions are similar to *evergreen broadleaf forest*, but LAI ground reference is not available for this land cover class. Again, misclassifications of GLC2000 can be excluded as a reason for the unrealistically high amount of LAI values below 1.5 in MOD15A2 because of low commission errors for this class (<2.5%, [45]).

For *deciduous woodland* and *deciduous shrubland*, CYCLOPES, GEOV1 and LSA-SAF LAI show relatively consistent distributions with peaks around LAI values of 2–3 (Figure 7(c,d)). MODIS LAI is shifted towards lower values, particularly for *deciduous woodlands*. These lower values of MOD15A2 are related to the decrease of LAI south of approximately 11°N (compare Figure 6(a)) which is obviously caused by remaining cloud contamination. For the *deciduous shrubland* class, only a single *in situ* dataset of 2005 is available (Donga, Table 3). Even though it has to be emphasized that a single *in situ* dataset cannot be representative for the whole land cover type, it can be noted that the ground measured LAI value of 1.8 generally fits to the LAI distributions of the investigated products.

In *croplands with open woody vegetation*, the LAI distributions peak between 1 and 3 (Figure 7(e)). The distribution of LSA-SAF LAI is narrow with hardly any data below 1 and above 3. MOD15A2, CYCLOPES and GEOV1 in contrast show a wider distribution with higher frequencies particularly for LAI values below 1.5. A similar situation is given for the drier agricultural class *cultivated and managed areas*. Here, LSA-SAF LAI values range in a narrow interval between 0.5 and 2.5 and maximum frequencies are found between an LAI of 1 and 2 (Figure 7(f)). In MOD15A2, CYCLOPES and GEOV1 products, the distribution is wider with LAI ranging between 0 and 3. A considerable fraction of data shows lower LAI values with peaks between 0 and 1.5 and GEOV1 and CYCLOPES

data show a second peak around an LAI of 2. Ground measurements of LAI are not available for the mentioned agricultural classes in West Africa.

The LAI distributions for the classes *sparse grassland* and *closed-open grassland* are relatively consistent for all products with peaks between 0 and 1 (Figure 7(g,h)). GEOV1 and CYCLOPES distributions show a second peak at LAI values of 1.5–2. The available *in situ* data for grasslands are in a similar range between LAI values of 0 and 2.5 (Table 3).
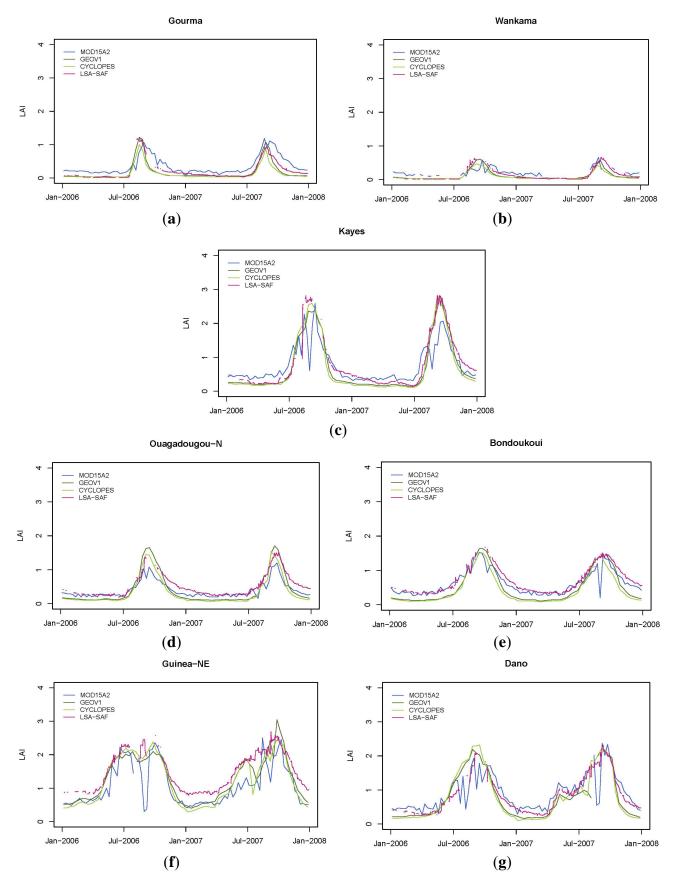
3.3. Temporal LAI Profiles

The temporal development of LAI during the years 2006 and 2007 at 13 selected sites (Table 2) is illustrated in Figure 8. The temporal profiles allow an assessment of the products' capabilities to capture the seasonality (phenology) of vegetation. Additionally, the temporal profiles allow for a comparison of the LAI magnitude over longer periods and of the smoothness of the time series. A smooth temporal course of LAI is typically expected as biomass production and leaf development are slow, incremental processes with only few exceptions of disturbances such as fire, flooding or rapid human land cover transformation [7].
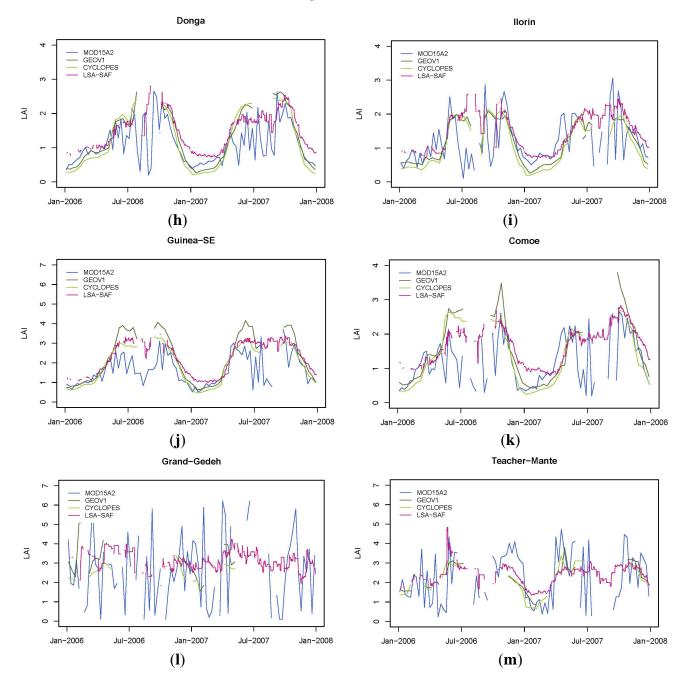
With regard to the adequate reproduction of phenological cycles, we find considerable spatial variations within the LAI datasets. The sites Gourma, Wankama, Kayes, Ouagadougou-N and Bondoukoui (Figure 8(a–e)) are located in the arid to semi-arid north of the study region and are characterized by a relatively low vegetation cover (*closed-open grassland*, *cultivated and managed areas*, *croplands with open woody vegetation*). For these sites, all considered LAI products depict the phenological phasing appropriately. Onset and peak of the vegetation phase are consistent over all datasets. Only for MOD15A2, the senescence phase is slightly retarded at the Gourma site. Guinea-NE, Dano, Donga, Ilorin, Guinea-SE, and Comoe (Figure 8(f–k)) are characterized by a semiarid to dry sub-humid climate and land cover is dominated by *deciduous shrubland*, and *deciduous woodland*. Here, MOD15A2 depicts the dry season of the *deciduous shrubland* and *deciduous woodland* classes, but during rainy season, time series are very shaky and do hardly describe the increase, peak and decrease of LAI during the vegetation phase (Figure 8(f–k)). LSA-SAF, CYCLOPES and GEOV1 LAI time series in contrast reproduce the typical alterations of rainy and dry seasons. However, CYCLOPES and GEOV1 show major data gaps during the vegetation phase for Donga, Guinea-SE, Comoe and Ilorin. This hinders delineating a maximum LAI magnitude for these sites. LSA-SAF LAI describes the seasonal course most consistently of all datasets. Even for the year 2006, where data gaps in LSA-SAF LAI are considerable, data is available for the peak of the vegetation phase.

However, LSA-SAF LAI shows slight break-ins during the vegetation phases for some sites (Donga, Comoe, Ilorin). For the sub-humid sites Grand Gedeh (*evergreen broadleaf forest*) and Teacher Mante (*mosaic forest / cropland*), only LSA-SAF LAI is able to provide an almost consistent picture of the seasonal LAI development (Figure 8(l–m)). Nevertheless, LSA-SAF time series are shakier than at the other sites and LAI break-ins are observable for Teacher Mante during the vegetation phase 2007. MOD15A2 LAI is extremely rugged for Grand Gedeh and Teacher Mante and GEOV1 and CYCLOPES are dominated by data gaps. Therefore, the latter three LAI time series do not support the delineation of any phenological development for these sub-humid sites.

Figure 8. Temporal profiles of MOD15A2, CYCLOPES, GEOV1 and LSA-SAF LAI for the selected focus sites (3 km × 3 km) and the years 2006 and 2007. The LAI plots are arranged according to the location of the sites from north to south and east to west.

(a)

(b)

(c)

(d)

(e)

(f)

(g)

Figure 8. *Cont.*

(h)

(i)

(j)

(k)

(l)

(m)

With respect to the smoothness of the temporal profiles, GEOV1 and CYCLOPES LAI time series show very good characteristics, with a single exception being the vegetation phase 2007 at the Guinea-NE site. MOD15A2 time series are relatively rugged when compared with the other products under investigation. One reason for the high noise in MODIS LAI could be the shorter temporal sampling interval (8 days) when compared to CYCLOPES and GEOV1 (30 days). However, given the enormous jumps of several LAI units within few weeks, the occurrence of extremely low values during the vegetation phase, and the comparably few data gaps also in obviously problematic periods and sites, it seems obvious that MOD15A2 data is heavily affected by residual cloud contamination. The profiles of LSA-SAF LAI shake at a high frequency but low amplitude. Here, noise seems to be indeed related to the daily sampling interval.

In terms of LAI magnitudes, CYCLOPES and GEOV1 exhibit lower dry season LAI values than LSA-SAF and MOD15A2, consistently over all sites. LSA-SAF LAI values are generally higher than CYCLOPES and GEOV1 LAI values at the start of the dry season but decrease continuously and approximately reach the level of the latter datasets at the end of the dry season. Given the dormancy of vegetation during the dry season, this slow decrease in LAI can hardly be explained by a phenological phenomenon but rather seems to be related to problems in LAI retrieval. For the vegetation phase, LAI magnitudes are in good agreement for all products at the sites Gourma, Wankama and Bondoukoui. For all other sites, vegetation phase LAI values are similar for GEOV1, CYCLOPES and LSA-SAF but MOD15A2 LAI values are either lower or significantly jump above and below the other time series. At Guniea-SE, GEOV1 is approximately one LAI unit above CYCLOPES and LSA-SAF. *In situ* measurements of 2005, 2001 and 2000 are available for Donga, Wankama and Gourma (Table 3). However, for these locations, the bi-annual plots (Figure 8) and the bi-annual *in situ* measurements at Gourma indicate an inter-annual variability of LAI. The magnitude of this variability is similar to the observed inter-product differences. This makes it impossible to reliably evaluate the product accuracies based on the available ground data.

4. Discussion

The presented intercomparison of the LAI products allows for an evaluation with regard to their applicability in regional land surface and climate modeling studies. Table 4 summarizes several criteria that are of interest in this context. Depending on the kind of application, the listed aspects will be of higher or lower relevance for a potential user. Table 4 enables users to base their decision on those criteria that are most crucial for a specific application.

A first aspect is the temporal coverage of the LAI product. GEOV1 and MOD15A2 provide the longest time series from 1999 and 2000 until today. As LSA-SAF data is only available since 2006, this dataset to date covers a relatively short period only. The temporal resolution of all LAI products is sufficient for many land surface and climate modeling studies. As biomass production and leaf development are usually slow processes, daily data on LAI is not imperative. The spatial resolution of LAI datasets however might be more crucial. Even though for climate models, the LSA-SAF resolution of 3 km is more than adequate, hydrological modeling or modeling of net primary productivity might require the higher spatial resolution of MOD15A2, GEOV1 and CYCLOPES. This is particularly relevant in landscapes like in West Africa where small-scaled, land use related vegetation patterns are common.

With respect to data gaps, LSA-SAF LAI shows best preconditions for temporally consistent analyses of LAI in West Africa. Except for the first year of data availability, 2006, data gaps account for less than 7%. In contrast to the other products, gaps do not accumulate during the rainy season here. A reason might be the higher temporal frequency of the SEVIRI observations (15 min) compared to the daily records of the near-polar orbiting SPOT-VGT and MODIS instruments, which increases the chances for cloud-free observations in tropical areas [47]. Among the LAI products derived from near-polar orbiting instruments, MOD15A2 shows best characteristics with respect to data gaps, particularly in the densely vegetated areas south of 10°N. Missing LAI values on barren or sparsely vegetated areas can be

considered less relevant for regional modeling studies. Vegetation cover is rather insignificant in these areas and its influence on water and energy fluxes is expected to be low.

However, when regarding the temporal profiles of LAI values, major problems become apparent for MOD15A2, particularly in the south of the study region. The extremely rugged time series and the occurrence of unrealistically low LAI values during the vegetative phase show that low data gap frequencies obviously go along with remaining cloud contamination in MOD15A2 data. The smooth time series of CYCLOPES and GEOV1 LAI in contrast indicate that in these products, the influence of clouds has been largely eliminated. However, persistent data gaps during the vegetation phase in the sub-humid zone of West Africa do not allow the delineation of vegetation structural properties at the peak of the vegetation phase from GEOV1 and CYCLOPES data either. LSA-SAF LAI data in contrast provides continuous information even for the rainy season in the south of the study region. The daily time series are slightly rugged, but temporal aggregation to 8- or 10-day time series could result in profiles of a smoothness that is comparable to the GEOV1 and CYCLOPES products.

Table 4. Summary of criteria evaluating the LAI datasets.

Criteria	GEOV1	CYCLOPES	MOD15A2	LSA-SAF
temporal coverage	+	+/−	+	−
temporal resolution	+	+	+	+
spatial resolution	+	+	+	+/−
data gaps				
arid to semi-arid zone	+	+/−	−	+
sub-humid zone	−	−	+	+
smoothness of temporal profiles				
arid to semi-arid zone	+	+	+/−	+
sub-humid zone	+	+	−	+
reproduction of phenological variations				
arid to semi-arid zone	+	+/−	+	+
sub-humid zone	+/−	+/−	−	+
Plausibility of LAI magnitudes				
barren & sparsely vegetated areas	+	+	+	+
savannas and agriculture	+	+	+	+
forests	−	−	+/−	+/−

A quantitative validation of LAI magnitudes in West Africa is not possible as no adequate number of LAI *in situ* measurements is available. Furthermore, the few existing ground surveys have been taken prior to the period of investigation when LSA-SAF LAI was not yet available. This temporal inconsistency between remote sensing products and *in situ* measurements is particularly critical in semi-arid areas where the inter-annual variability of vegetation is high. However, based on LAI magnitudes known from *in situ* measurements of East African *evergreen broadleaf forests* [13], it can be concluded that MODIS shows less saturation and provides more realistic (*i.e.*, higher) values for this land cover type than the other products, as long as cloud contamination is not present. Still, it should be mentioned that [11] observed an overestimation of LAI in the MODIS product for the Amazonian forests which they interpreted as an overcompensation of the saturation effect. In general however, the usability of MODIS LAI in *evergreen broadleaf forest* regions of West Africa is

diminished by the fact that both the statistical distributions and the rugged temporal profiles also indicate a considerable number of unrealistically low MODIS LAI values within this land cover type. In general, all products showed good pixel-based agreement for LAI values below 2. For higher LAI values, MODIS showed mainly negative deviations from other products. The respective LAI maps indicate that MODIS provides lower values than the other products particularly at the fringes of cloud-related data gaps. The lower MOD15A2 magnitudes are thus likely to be caused by remaining cloud contamination in these areas.

5. Conclusions

In this study, four freely available LAI products were intercompared with respect to their applicability in regional modeling studies for West Africa. However, due to a current lack in sufficient and representative ground measurements of LAI, our analyses cannot present a proper validation of the selected products. For reliable, quantitative validation exercises, sampling rates of the time-demanding *in situ* measurements of LAI will need to be increased. Furthermore, these measurements will need to cover typical land cover classes and seasonal variations in a representative way, not only at global but also at regional scale.

The presented comparative analyses indicated similar and good characteristics of the CYCLOPES and the GEOV1 LAI products. LAI magnitudes are in good agreement (RMSE: 0.24) and seem adequate for the predominant land cover types of West Africa, except for some obvious underestimation for *evergreen broadleaf forests*. More than one quarter of this land cover class shows LAI values below 1.5. Major problems generally arise in the sub-humid, frequently clouded areas in the south of the study region. Here, data gaps typically affect more than 50% of the CYCLOPES and GEOV1 LAI time series and mainly accumulate during the vegetative due to persistent cloud cover. Moderate advantages of GEOV1 when compared to CYCLOPES were found in arid to semi-arid regions with respect to data gaps and realistic description of phenology. Also the longer temporal coverage of GEOV1 might be beneficial for a number of applications.

MOD15A2 LAI provides similar characteristics with respect to temporal coverage and spatio-temporal resolution. Data gaps are less frequent than in the GEOV1 and CYCLOPES products and only in rare cases missing data exceed 70%, even in the cloud affected south. However, in these more humid zones, MOD15A2 shows deficits when regarding the smoothness of temporal profiles, and the ability to reproduce vegetation phenology. For clear-sky observations, MOD15A2 obviously provide most realistic LAI magnitudes in forested areas but frequent residual cloud contamination in the dataset seems to be a particular problem of this dataset.

LSA-SAF LAI shows good characteristics for most of the considered criteria. Drawbacks for some applications might be the short temporal coverage since 2006 and the relatively coarse spatial resolution of approximately 3 km. Based on data acquired from a geostationary platform, the LSA-SAF product shows a fraction of data gaps typically below 7%. Thus, the LSA-SAF LAI bears great potential to provide crucial information for the particularly critical periods of high cloud coverage and, at the same time, major vegetation activity.

The complementary strengths of GEOV1 or CYCLOPES and LSA-SAF LAI could lead to an optimized LAI time series when exploiting the advantages of both datasets. In this case, future research

efforts could focus on data fusion approaches that accept the differences in spatial resolutions, and consider that LSA-SAF LAI data is not available prior to 2006.

References

1. Myneni, R.B.; Ramakrishna, R.; Nemani, R.; Running, S.W. Estimation of global leaf area index and absorbed par using radiative transfer models. *IEEE Trans. Geosci. Remote Sens.* **1997**, *35*, 1380–1393.
2. Paeth, H.; Born, K.; Girmes, R.; Podzun, R.; Jacob, D. Regional climate change in tropical and Northern Africa due to greenhouse forcing and land use changes. *J. Clim.* **2009**, *22*, 114–132.
3. Wagner, S.; Kunstmann, H.; Bardossy, A.; Conrad, C.; Colditz, R.R. Water balance estimation of a poorly gauged catchment in West Africa using dynamically downscaled meteorological fields and remote sensing information. *Phys. Chem. Earth* **2009**, *34*, 225–235.
4. Wisskirchen, K. Modellierung der Regionalen CO2-Aufnahme durch Vegetation. Ph.D. Thesis, Friedrich-Wilhelm University, Bonn, Germany, 2005; p. 124.
5. Hagemann, S. *An Improved Land Surface Parameter Dataset for Global and Regional Climate Models*; MPI Report 336; MPI: Hamburg, Germany, 2002; Volume 336.
6. Garrigues, S.; Lacaze, R.; Baret, F.; Morisette, J.T.; Weiss, M.; Nickeson, J.E.; Fernandes, R.; Plummer, S.; Shabanov, N.V.; Myneni, R.B.; *et al.* Validation and intercomparison of global Leaf Area Index products derived from remote sensing data. *J. Geophys. Res.* **2008**, *113*, G02028.
7. Weiss, M.; Baret, F.; Garrigues, S.; Lacaze, R. LAI and fAPAR CYCLOPES global products derived from VEGETATION-Part 2: Validation and comparison with MODIS collection 4 products. *Remote Sens. Environ.* **2007**, *110*, 317–331.
8. Hill, M.J.; Senarath, U.; Lee, A.; Zeppel, M.; Nightingale, J.M.; Williams, R.J.; McVicar, T.R. Assessment of the MODIS LAI product for Australian ecosystems. *Remote Sens. Environ.* **2006**, *101*, 495–518.
9. Fensholt, R.; Sandholt, I.; Rasmussen, M.S. Evaluation of MODIS LAI, fAPAR and the relation between fAPAR and NDVI in a semi-arid environment using *in situ* measurements. *Remote Sens. Environ.* **2004**, *91*, 490–507.
10. Fang, H.; Wei, S.; Liang, S. Validation of MODIS and CYCLOPES LAI products using global field measurement data. *Remote Sens. Environ.* **2012**, *119*, 43–54.

11. Aragao, L.E.O.C.; Shimabukuro, Y.E.; Espirito-Santo, F.D.B.; Williams, M. Spatial validation of the collection 4 MODIS LAI product in eastern Amazonia. *IEEE Trans. Geosci. Remote Sens.* **2005**, *43*, 2526–2534.

12. Shimabukuro, Y.E.; Aragao, L.E.O.C.; Espirito-Santo, F.D.B.; Williams, M. Combining Landsat ETM+ and Terrain Data for Scaling up Leaf Area Index (LAI) in Eastern Amazon: An Intercomparison with MODIS Product. In Proceedings of 2004 IEEE International Geoscience and Remote Sensing Symposium (IGARSS'04), Anchorage, AK, USA, 20–24 September 2004; Volume 3, pp. 2050–2053.

13. Kraus, T. Ground-Based Validation of the MODIS Leaf Area Index Product for East African Rain Forest Ecosystems. Ph.D. Thesis, Friedrich-Alexander Universität Erlangen-Nürnberg, Erlangen, Germany, 2008.

14. Cohen, W.B.; Maiersperger, T.K.; Turner, D.P.; Ritts, W.D.; Pflugmacher, D.; Kennedy, R.E.; Kirschbaum, A.; Running, S.W.; Costa, M.; Gower, S.T. MODIS land cover and LAI collection 4 product quality across nine sites in the western hemisphere. *IEEE Trans. Geosci. Remote Sens.* **2006**, *44*, 1843–1857.

15. Pandya, M.R.; Singh, R.P.; Chaudhari, K.N.; Bairagi, G.D.; Sharma, R.; Dadhwal, V.K.; Parihar, J.S. Leaf area index retrieval using IRS LISS-III sensor data and validation of the MODIS LAI product over central India. *IEEE Trans. Geosci. Remote Sens.* **2006**, *44*, 1858–1865.

16. De Kauwe, M.G.; Disney, M.I.; Quaife, T.; Lewis, P.; Williams, M. An assessment of the MODIS collection 5 leaf area index product for a region of mixed coniferous forest. *Remote Sens. Environ.* **2011**, *115*, 767–780.

17. Fang, H.; Li, W.; Myneni, R.B. The impact of Potential land cover misclassification on MODIS Leaf Area Index (LAI) estimation: A statistical perspective. *Remote Sens.* **2013**, *5*, 830–844.

18. Baret, F.; Weiss, M. *Towards an Operational GMES Land Monitoring Core Service—BioPar Methods Compendium-LAI, FAPAR, F COVER NDVI, Issue 1.5*; Geoland 2. EC Proposal Reference No. FP-7-218795; 2010. Available online: http://web.vgt.vito.be/documents/BioPar/g2-BP-RP-BP038-ATBD_VegetationVariables_INRA-I1.5.pdf (accessed on 06 March 2013).

19. Land-SAF Product User Manual Vegetation Parameters (FVC, LAI, FAPAR), Version 2.1; 2008. Avaliable online: http://landsaf.meteo.pt/GetDocument.do?id=300 (accessed on 06 March 2013).

20. Verger, A.; Camacho, F.; García-Haro, F.J.; Meliá, J. Prototyping of Land-SAF leaf area index algorithm with VEGETATION and MODIS data over Europe. *Remote Sens. Environ.* **2009**, *113*, 2285–2297.

21. Privette, J.L.; Myneni, R.B.; Knyazikhin, Y.; Mukelabai, M.; Roberts, G.; Tian, Y.; Wang, Y.; Leblanc, S.G. Early spatial and temporal validation of MODIS LAI product in the Southern Africa Kalahari. *Remote Sens. Environ.* **2002**, *83*, 232–243.

22. Baret, F.; Hagolle, O.; Geiger, B.; Bicheron, P.; Miras, B.; Huc, M.; Berthelot, B.; Nino, F.; Weiss, M.; Samain, O.; *et al.* LAI, fAPAR and fCover CYCLOPES global products derived from VEGETATION. Part 1: Principles of the algorithm. *Remote Sens. Environ.* **2007**, *110*, 275–286.

23. Knyazikhin, Y.; Glassy, J.; Privette, J.L.; Tian, Y.; Lotsch, A.; Zhang, Y.; Wang, Y.; Morisette, J.T.; Votava, P.; Myneni, R.B.; *et al.* MODIS Leaf Area Index (LAI) and Fraction of Photosynthetically Active Radiation Absorbed by Vegetation (FPAR) Product (MOD15) Algorithm Theoretical Basis Document; Version 4.0, 1999. Available online: http://modis.gsfc.nasa.gov/data/atbd/atbd_mod15.pdf (accessed on 06 March 2013).

24. Myneni, R.B.; Hoffman, S.; Knyazikhin, Y.; Privette, J.L.; Glassy, J.; Tian, Y.; Wang, Y.; Song, X.; Zhang, Y.; Smith, G.R.; *et al.* Global products of vegetation leaf area and fraction absorbed PAR from year one of MODIS data. *Remote Sens. Environ.* **2002**, *83*, 214–231.

25. Bartholomé, E.; Belward, A.S. GLC2000: A new approach to global land cover mapping from Earth observation data. *Int. J. Remote Sens.* **2005**, *26*, 1959–1977.

26. Pôle d'Observation des Surfaces continentals par Telédétection (POSTEL). Available online: http://postel.mediasfrance.org/ (accessed on 06 March2013).

27. Jacquemoud, S.; Verhoef, W.; Baret, F.; Bacour, C.; Zarco-Tejada, P.J.; Asner, G.P.; Francois, C.; Ustin, S.L. PROSPECT+SAIL models: A review of use for vegetation characterization. *Remote Sens. Environ.* **2009**, *113*, 556–566.

28. Land Processes Distributed Active Archive Center (LP DAAC). Available online: https://lpdaac.usgs.gov/ (accessed on 06 March 2013).

29. Geoland2. Operational Monitoring Services for our Changing Environment. Available online: http://www.gmes-geoland.info/ (accessed on 06 March 2013).

30. Land Surface Analysis Satellite Applications Facility (LSA SAF). Available online: https://landsaf.meteo.pt/ (accessed on 06 March 2013).

31. NASA Collection 5 LAI/FPAR Changes. Available online: http://landweb.nascom.nasa.gov/QA_WWW/forPage/C005_Changes_LAI_FPAR.pdf (accessed on 06 March 2013).

32. Baret, F.; Morissette, J.T.; Fernandes, R.A.; Champeaux, J.L.; Myneni, R.B.; Chen, J.; Plummer, S.; Weiss, M.; Bacour, C.; Garrigues, S.; *et al.* Evaluation of the representativeness of networks of sites for the global validation and intercomparison of land biophysical products: Proposition of the CEOS-BELMANIP. *IEEE Trans. Geosci. Remote Sens.* **2006**, *44*, 1794–1803.

33. Roujean, J.L.; Lacaze, R. Global mapping of vegetation parameters from POLDER multiangular measurements for studies of surface-atmosphere interactions: A pragmatic method and its validation. *J. Geophys. Res.* **2002**, *107*, ACL 6-1–ACL 6-11.

34. Chen, J.M.; Menges, C.H.; Leblanc, S.G. Global mapping of foliage clumping index using multi-angular satellite data. *Remote Sens. Environ.* **2005**, *97*, 447–457.

35. Ge, J.; Torbick, N.; Qi, J. Biophysical evaluation of land-cover products for land–climate modeling. *Earth Interact.* **2009**, *13*, 1–16.

36. Niklaus, M.; Tum, M.; Günther, K. Modeling Carbon Sinks and Sources in semi-arid Environments for a Land Degradation Assessment Approach. In Proceedings of the 24th International Conference on Informatics for Environmental Protection, Cologne/Bonn, Germany, 8–10 October 2010; pp. 648–656.

37. Niklaus, M.; Tum, M.; Günther, K. NPP Modelling for Biomass Energy Estimations of South Africa. In Proceedings of the 8th AARSE Conference, Addis Ababa, Ethiopia, 25–29 October 2010.

38. Jung, M.; Henkel, K.; Herold, M.; Churkina, G. Exploiting synergies of global land cover products for carbon cycle modeling. *Remote Sens. Environ.* **2006**, *101*, 534–553.

39. Giri, C.; Zhu, Z.; Reed, B. A comparative analysis of the Global Land Cover 2000 and MODIS land cover data sets. *Remote Sens. Environ.* **2005**, *94*, 123–132.

40. Committee on Earth Observation Satellites. CEOS Cal/Val Portal, BELMANIP 2. Available online: http://calvalportal.ceos.org/cvp/web/olive/site-description (accessed on 06 June 2013).

41. The VALERI Project (Validation of Land European Remote sensing Instruments); 2011. Available online: http://w3.avignon.inra.fr/valeri/Meeting_Reports/Davos_2007/ Rossello_Davos_VALERI.pdf (accessed on 06 March 2013).

42. Wang, Y.; Tian, Y.; Zhang, Y.; El-Saleous, N.; Knyazikhin, Y.; Vermote, E.; Myneni, R.B. Investigation of product accuracy as a function of input and model uncertainties: Case study with SeaWiFS and MODIS LAI/FPAR algorithm. *Remote Sens. Environ.* **2001**, *78*, 299–313.

43. Asner, G.P.; Scurlock, J.M.O.; Hicke, J.A. Global synthesis of leaf area index observations: implications for ecological and remote sensing studies. *Glob. Ecol. Biogeogr.* **2003**, *12*, 191–205.

44. Lacaze, R. *CSP—Algorithm Theoretical Basis Document (ATBD) WP 8312-Customisation for LAI, fAPAR, fcover and Albedo*; 2004. Available online: http://toyo.mediasfrance.org/IMG/pdf/ CSP-0350-ATBD_CustomizedLAI_FAPAR_FCover_Albedo-I1.00.pdf (accessed on 6 March 2013).

45. Mayaux, P.; Eva, H.; Gallego, J.; Strahler, A.H.; Herold, M.; Agrawal, S.; Naumov, S.; De Miranda, E.E.; Di Bella, C.M.; Ordoyne, C.; *et al.* Validation of the global land cover 2000 map. *IEEE Trans Geosci. Remote Sens.* **2006**, *44*, 1728–1739.

46. Food and Agriculture Organization of the United Nations (FAO-UN). FAOSTAT. Available online: http://faostat3.fao.org/home/index.html#HOME (accessed on 06 March 2013).

47. Fensholt, R.; Anyamba, A.; Huber, S.; Proud, S.R.; Tucker, C.J.; Small, J.; Pak, E.; Rasmussen, M.O.; Sandholt, I.; Shisanya, C. Analysing the advantages of high temporal resolution geostationary MSG SEVIRI data compared to Polar Operational Environmental Satellite data for land surface monitoring in Africa. *Int. J. Appl. Earth Obs. Geoinf.* **2011**, *13*, 721–729.